

See discussions, stats, and author profiles for this publication at: <https://www.researchgate.net/publication/263961107>

Alternating Electron Donor–Acceptor Conjugated Polymers Based on Modified Naphthalene Diimide Framework: The Large Enhancement of p-Type Semiconducting Performance upon Solvent Vap...

ARTICLE *in* MACROMOLECULES · JULY 2013

Impact Factor: 5.8 · DOI: 10.1021/ma4009803

CITATIONS

8

READS

26

7 AUTHORS, INCLUDING:



Guanxin Zhang

Chinese Academy of Sciences

130 PUBLICATIONS 4,281 CITATIONS

SEE PROFILE



Zitong Liu

Chinese Academy of Sciences

35 PUBLICATIONS 277 CITATIONS

SEE PROFILE



Xin Chen

Fourth Military Medical University

43 PUBLICATIONS 204 CITATIONS

SEE PROFILE



Jianguo Wang

Gannan Normal University

19 PUBLICATIONS 230 CITATIONS

SEE PROFILE

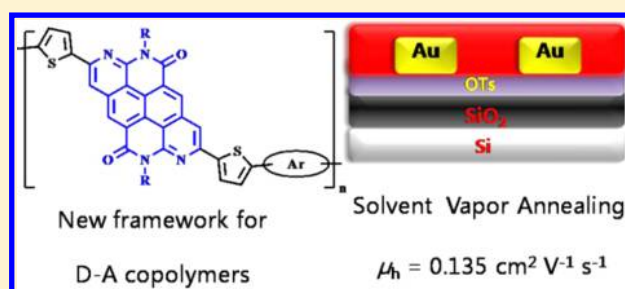
Alternating Electron Donor–Acceptor Conjugated Polymers Based on Modified Naphthalene Diimide Framework: The Large Enhancement of p-Type Semiconducting Performance upon Solvent Vapor Annealing

Yonghai Li, Guanxin Zhang,* Zitong Liu, Xin Chen, Jianguo Wang, Chong'an Di, and Deqing Zhang*

Beijing National Laboratory for Molecular Sciences, Organic Solids Laboratory, Institute of Chemistry, Chinese Academy of Sciences, Beijing 100190, China

S Supporting Information

ABSTRACT: Three new alternating conjugated D–A polymers **P1**, **P2**, and **P3** are reported. They entail a new expanded conjugated framework that is derived from naphthalene diimide (NDI) possesses planar structure and moderate electron-accepting capacity. Benzo[1,2-*b*:4,5-*b'*]dithiophene with alkoxy and alkyl chains and thiophene are the respective electron-donating moieties. These conjugated polymers are thermally stable under 325 °C based on their TGA data. **P1**, **P2**, and **P3** exhibit similar HOMO (ca. –5.39 to –5.43 eV) and LUMO (ca. –3.58 to –3.59 eV) energies according to their absorption spectra and redox potentials. The results reveal that **P1**, **P2**, and **P3** can be solution-processed, and the resulting OTFTs exhibit hole mobilities in the range of $(1.3\text{--}3.0) \times 10^{-3} \text{ cm}^2 \text{ V}^{-1} \text{ s}^{-1}$ and current on/off ratios of $10^5\text{--}10^7$ after conventional thermal annealing. Notably, hole mobilities of thin films of **P2** and **P3** increase to 0.024 and $0.135 \text{ cm}^2 \text{ V}^{-1} \text{ s}^{-1}$, respectively, upon solvent vapor annealing.



INTRODUCTION

Conjugated polymers that exhibit electronic semiconducting behaviors have received increasing attentions for the past decades.¹ This is because (i) they show promising applications in light-emitting diodes,² organic photovoltaics (OPVs),³ integrated transistors, and other areas⁴ and (ii) they can be solution-processed to enable the manufacture of flexible, low-cost, and large-area devices. Recently, the strategy of incorporating donor (D) and acceptor (A) units into the polymer backbone has proven to be very effective in improving device performances by taking advantage of intermolecular donor and acceptor interactions. A number of alternating D–A conjugated polymers have been designed and investigated for optoelectronic materials. Among them p-type, n-type, and even ambipolar semiconducting conjugated polymers were reported with carrier mobilities higher than $1.0 \text{ cm}^2 \text{ V}^{-1} \text{ s}^{-1}$.^{5,6} These D–A conjugated polymers were also successfully utilized to fabricate OPVs with power conversion efficiency up to 7%.^{7,8} Nevertheless, new D–A conjugated polymers with different frameworks are still desirable for optoelectronic materials of high performance and investigations on the structure–property correlations.

Various electron accepting moieties have been utilized to construct conjugated D–A polymers for semiconducting and photovoltaic materials.^{9–13} Among them naphthalene diimide (NDI) is widely used as electron accepting units within alternating D–A conjugated polymers. For instance, Facchetti,

Luscombe, and their co-workers reported a series of alternating NDI–thiophene polymers, and the resulting OTFTs based on **PNDI1** (Scheme 1) exhibited electron mobilities up to $0.85 \text{ cm}^2 \text{ V}^{-1} \text{ s}^{-1}$ under ambient conditions.¹⁴ Interestingly, **PNDI2** (Scheme 1) with alternating electron-donating dialkoxybithiophene and NDI moieties were found to show ambipolar semiconducting behavior with electron and hole mobilities as high as 0.04 and $0.003 \text{ cm}^2 \text{ V}^{-1} \text{ s}^{-1}$, respectively.¹⁵ In addition, two NDI relevant conjugated polymers [poly-(benzobisimidazobenzophenanthroline) (BBL) and its analogue BBB (see Scheme 1)] were reported to exhibit n-type semiconducting property with electron mobility up to $0.1 \text{ cm}^2 \text{ V}^{-1} \text{ s}^{-1}$.¹⁶

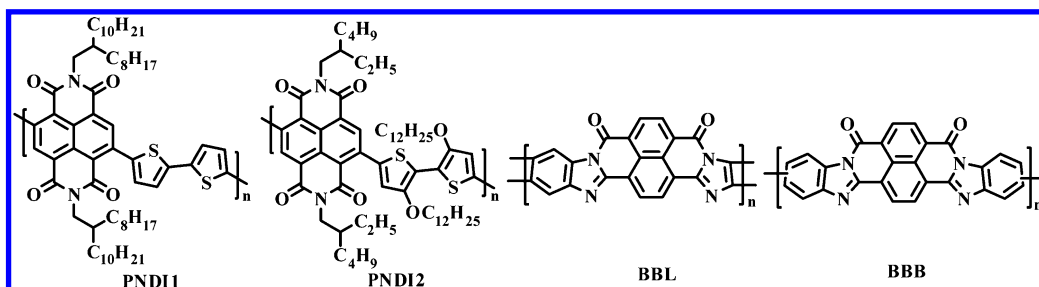
Some of us have very recently disclosed a new chemical modification at the shoulder position of NDI leading to a new expanded conjugated framework (see Scheme 2) that possesses planar structure and moderate electron-accepting capacity.¹⁷ In this paper we report new alternating conjugated polymers **P1**, **P2**, and **P3** which contain this new conjugated framework (as electron-accepting moieties) and the respective electron-donating moieties (benzo[1,2-*b*:4,5-*b'*]dithiophene with alkoxy and alkyl chains, and thiophene). The results reveal that **P1**, **P2**, and **P3** (see Scheme 3) can be solution-processed, and the

Received: May 14, 2013

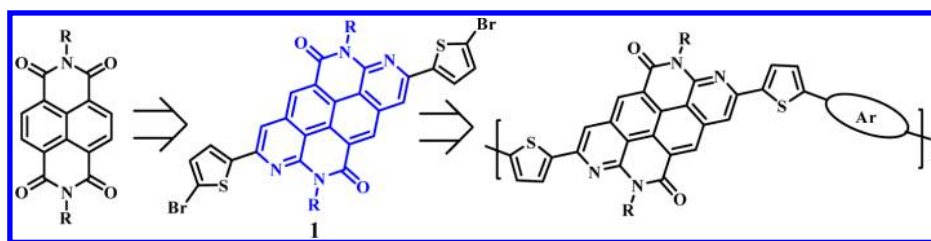
Revised: July 4, 2013

Published: July 12, 2013

Scheme 1. Representative NDI-Based Conjugated Polymers



Scheme 2. Transformation of NDI into a New Expanded Conjugated Framework and the Building Block for New D–A Conjugated Polymers



resulting OTFTs exhibit hole mobilities in the range of $(1.3\text{--}3.0) \times 10^{-3} \text{ cm}^2 \text{ V}^{-1} \text{ s}^{-1}$ and current on/off ratios of $10^5\text{--}10^7$ after conventionally thermal annealing. Notably, hole mobilities of thin films of **P2** and **P3** increase to 0.024 and 0.135 $\text{cm}^2 \text{ V}^{-1} \text{ s}^{-1}$, respectively, upon solvent vapor annealing. Furthermore, **P1**, **P2**, and **P3** exhibit relatively broad and strong absorptions, and accordingly these conjugated polymers may find potential applications in OPVs.

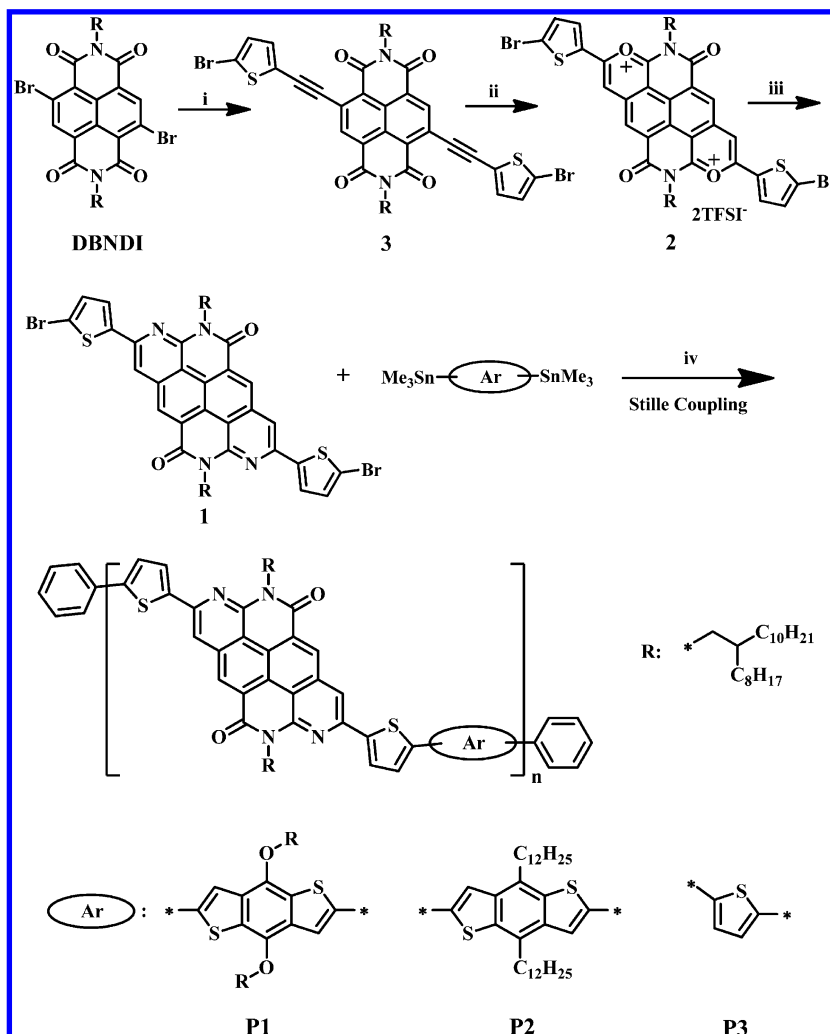
Synthesis and Characterization. **P1**, **P2**, and **P3** were prepared by utilizing the Stille coupling reaction between compound **1** and the respective bis-trimethylstannane compounds as depicted in Scheme 3. The synthesis of **1** started from dibromo-NDI (DBNDI), which was transformed into compound **3** after reaction with ((5-bromothiophen-2-yl)ethynyl)copper in DMSO according to previous report.¹⁸ Compound **3** was allowed to react with TFSIH [bis-(trifluoromethane) sulfonamide] under a nitrogen atmosphere to afford **2** as green solids which were used for next step without further purification. As reported earlier,¹⁹ **2** was formed via the intramolecular cyclization involving ethynyl and imide-carbonyl groups. Compound **1** was yielded after further treatment of the solution of **2** in dry methanol with $\text{NH}_3 \cdot \text{H}_2\text{O}$ under reflux in 52% yield based on **3**. The Stille coupling of **1** with the respective bis-trimethylstannane compounds [4,8-bis((2-octyldodecyl)oxy)benzo[1,2-*b*:4,5-*b'*]-dithiophene-2,6-diyl)bis(trimethylstannane), 4,8-didodecyl-2,6-bis(trimethylstannyl)benzo[1,2-*b*:4,5-*b'*]dithiophene, and 2,5-bis(trimethylstannyl)thiophene] was successfully carried out in the presence of $\text{Pd}_2(\text{dba})_3$ and $\text{P}(o\text{-toly})_3$ as catalyst and ligand, respectively. Finally, tributyl(phenyl)stannane and bromobenzene were added separately to each polymerization reaction to end-cap **P1**, **P2**, and **P3**.

P1, **P2**, and **P3** were purified by precipitation from methanol for several times, followed by Soxhlet extraction. For **P1** and **P2**, the precipitates were extracted with methanol, hexane, and acetone, in sequence, to remove the remaining monomers and oligomers. For **P3**, however, the solid samples after Soxhlet extraction with methanol, hexane, acetone, and chloroform were mixed with 50 mL of 1,2-dichlorobenzene (*o*-DCB), and

the resulting suspension was heated to 100 °C and stirred for 12 h; then, the 1,2-dichlorobenzene solution was separated, and methanol was added, leading to precipitation of **P3**.

P1 and **P2** are highly soluble (>50 mg/mL) in common organic solvents such as chloroform, tetrahydrofuran, toluene, and *o*-DCB at room temperature because of the presence of long and branched alkyl chains. In comparison, **P3** shows extremely poor solubility in common solvents at room temperature, but it can be dissolved in *o*-DCB at high temperature; for instance, the concentration of **P3** can reach ca. 10 mg/mL in *o*-DCB at 100 °C. The molecular weights M_n (number-average molecular weight) and M_w (weight-average molecular weight) as well as polydispersity index ($\text{PDI} = M_w/M_n$) of **P1**, **P2**, and **P3** were determined by gel permeation chromatography (GPC) at 150 °C using polystyrenes as standards with 1,2,4-trichlorobenzene as the eluent. As listed in Table 1, **P1**, **P2**, and **P3** possess relatively high M_n and M_w values ranging from 28.6 to 29.2 kg mol^{-1} and 56.6 to 94.2 kg mol^{-1} , respectively, with PDI of 1.9–3.3. TGA data (see Figure S1) reveal that **P1**, **P2**, and **P3** exhibit good thermal stability with thermal decomposition temperatures (T_d) above 325 °C at 5% weight loss under nitrogen. Moreover, **P1**, **P2**, and **P3** show no detectable thermal transitions up to 300 °C based on DSC data (see Figure S2).

HOMO/LUMO Energies Based on Absorption Spectra and Redox Potentials. The absorption spectra of **P1**, **P2** and **P3** as well as their thin films were measured. As depicted in Figure 1a the solutions of **P1** and **P2** exhibit almost identical absorptions in the range 380 nm–610 nm with the maxima and shoulder absorptions around 490 nm 517 nm, respectively. In comparison, the absorption spectrum of **P3** in solution is red-shifted; it absorbs strongly at 508 nm with an absorption shoulder around 560 nm. This may be understood as follows: 1) the long alkyl chains connecting to the respective electron donating moieties within **P1** and **P2** may induce the polymer backbones to be nonplanar, and as a result the conjugation degree along the polymer backbones of **P1** and **P2** may be reduced; 2) For **P3**, however, the electron donating moieties do not possess alkyl chains and thus interactions due to side alkyl

Scheme 3. Chemical Structures and Synthetic Approach to P1, P2, and P3^a

^aReactants and conditions: (i) ((5-bromothiophen-2-yl)ethynyl)copper, DMSO, 130 °C, 2.0 h, 68%; (ii) CH₂Cl₂, TFSIH [bis(trifluoromethane) sulfonamide], rt, 4.0 h; (iii) CH₃OH, NH₃·OH, reflux, 1.0 h, 52% based on 3; (iv) Pd₂(dba)₃, P(*o*-tolyl)₃, toluene or chlorobenzene, 110 °C, 48 h, followed by addition of tributyl(phenyl)stannane (refluxing for 2.0 h) and bromobenzene (refluxing for an additional 2.0 h).

Table 1. Decomposition Temperatures and Molecular Weights of P1, P2, and P3

polymers	<i>T</i> _d ^a (°C)	<i>M</i> _n (kg mol ⁻¹)	<i>M</i> _w (kg mol ⁻¹)	PDI
P1	327	28.6	82.5	2.9
P2	342	28.6	94.2	3.3
P3	377	29.2	56.6	1.9

^aReported as the temperature with 5% weight loss.

chains are comparably weak; accordingly, the interactions among the electron donating and accepting moieties may be enhanced leading to absorptions in long-wavelength region;¹⁵ 3) P3 shows poor solubility of at room temperature, thus aggregation due to intermolecular π - π stacking may occur for P3 in solution and such intermolecular interaction may also contribute to the absorption red-shifts for P3.

Compared to those in solutions, the absorption spectra of the thin films of P1–P3 are slightly red-shifted. For instance, the absorption band at 487 nm in solution is shifted to 495 nm for the thin film of P1. Such absorption spectral shifts are likely owing to the intermolecular interactions within thin films which may entail the electron donor and acceptor interactions. Based

on the respective onset absorptions of thin films of P1, P2, and P3, the optical bandgaps of P1, P2, and P3 were estimated to be 1.97, 1.91, and 1.89 eV, respectively (see Table 2). Obviously, P3 possesses a smaller bandgap. This may be attributed to the fact that the electron-donating and -accepting moieties along the backbone of P3 are strongly interacted as discussed above. Moreover, intermolecular π - π stacking can induce red-shift of the absorption spectrum of thin film of P3 and thus further narrow the bandgap. Nevertheless, the absorption maxima of P1, P2, and P3 are blue-shifted compared to that of PNDI1 (see Scheme 1).¹⁴

As depicted in Figure 1b, P1, P2, and P3 exhibit irreversible oxidation waves around 1.25, 1.18, and 1.16 V, respectively.²⁰ P1 shows an irreversible reduction wave around -0.95 V, whereas P2 and P3 possess quasi-reversible reduction waves around -0.95 and -0.93 V, respectively. As listed in Table 2, HOMO/LUMO energies of P1, P2, and P3 were estimated based on their respective onset oxidation and reduction potentials. HOMO and LUMO energies of P1, P2, and P3 are around -5.40 and -3.60 eV, respectively. Thus, hole injection from gold ($\phi = 5.1$ eV) electrodes into P1, P2, and P3 is expected to be favorable. Compared to that of PNDI1 (see

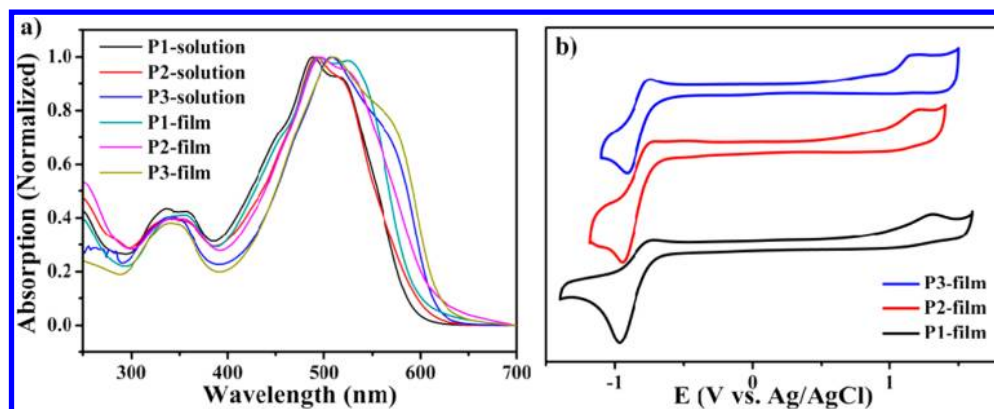


Figure 1. (a) Normalized UV-vis spectra for **P1**–**P3** in solutions (1.0×10^{-5} M, in CHCl_3 for **P1** and **P2**, in *o*-DCB for **P3**) and thin films. (b) Thin film cyclic voltammograms of the polymers. The measurements were conducted in acetonitrile at a scan rate of 100 mV/s with Bu_4NPF_6 (0.1 mol/L) as electrolyte. The thin films were prepared by volatilizing polymer solutions on the working electrode (in chloroform for **P1** and **P2**, in *o*-DCB for **P3**).

Table 2. Absorption, Electrochemical, HOMO/LUMO Energies and Band Gaps of **P1**, **P2**, and **P3**

compd	λ_{max}^a (nm) (ϵ_{max}^b $\text{M}^{-1} \text{cm}^{-1}$)		$E_{\text{onset}}^{\text{ox}}$ (V)	$E_{\text{onset}}^{\text{red}}$ (V)	HOMO ^c (eV)	LUMO ^c (eV)	E_g^{cv} (V)	$E_g^{\text{opt d}}$ (V)
	solution	film						
P1	487 (117 400)	495	1.00	−0.83	−5.41	−3.58	1.83	1.97
	517 (108 800)	526						
P2	492 (122 100)	495	1.02	−0.82	−5.43	−3.59	1.84	1.91
	517 (111 800)	526						
P3	508 (102 000)	512	0.98	−0.82	−5.39	−3.59	1.80	1.89
	561 (74 600)	565						

^aMeasured in CHCl_3 for **P1** and **P2**, in *o*-DCB for **P3** with a concentration of 1.0×10^{-5} M of the respective repeating units. ^bMolar extinction coefficient (ϵ_{max} $\text{M}^{-1} \text{cm}^{-1}$). ^cEstimated with the equations $\text{HOMO} = -(E_{\text{onset}}^{\text{ox}} + 4.41)$ eV and $\text{LUMO} = -(E_{\text{onset}}^{\text{red}} + 4.41)$ eV. ^dCalculated based on the onset absorption data.

Scheme 1),¹⁴ LUMO energies of **P1**, **P2**, and **P3** are relatively higher. This is in agreement with the fact that the electron accepting moiety within **P1**, **P2**, and **P3** is weaker than NDI in terms of electron-accepting ability.

Thin-Film OFETs. The semiconducting behaviors of **P1**, **P2**, and **P3** were investigated by characterizing OFETs with their thin films. The OFETs with bottom-gate and bottom-contact (BGBC) geometry were fabricated with conventional techniques (see Supporting Information). Solutions of **P1** (in chloroform), **P2** (in chloroform), and **P3** (in *o*-DCB at 100 °C) were spin-coated to form the respective thin films onto the OTS (*n*-octadecyltrichlorosilane)-modified SiO_2 (300 nm) surfaces, and drain-source (D-S) gold contacts were fabricated by photolithography. The as-prepared thin films of **P1**, **P2**, and **P3** all exhibit p-type semiconducting behaviors as anticipated from their HOMO/LUMO energy levels. Their hole mobilities are in the range of 2.2×10^{-4} – $4.0 \times 10^{-4} \text{ cm}^2 \text{ V}^{-1} \text{ s}^{-1}$ based on their transfer and output characteristics. Efforts were made to improve their semiconducting properties by both thermal and solvent vapor annealing. The thermal annealing was accomplished by leaving the thin films in a vacuum chamber for 1.0 h at each temperature. As listed in Table S1, hole mobilities of their thin films were enhanced (but not significantly) by increasing the annealing temperature from 25 to 140 °C, reaching 1.3×10^{-3} , 2.1×10^{-3} , and $3.0 \times 10^{-3} \text{ cm}^2 \text{ V}^{-1} \text{ s}^{-1}$ for thin films of **P1**, **P2**, and **P3**, respectively. This may be probably owing to the fact that rearrangements of conjugated polymer chains within thin films of **P1**, **P2**, and **P3** are not feasible even at high annealing temperature because of relatively high molecular weights (see Table 1).

The solvent vapor annealing was completed by carefully putting the thin films in a sealed glass containing 1.0 mL of different solvents at the bottom to generate solvent vapors for 24 h; then the films were left in a vacuum chamber at 80 °C for 1.0 h to completely remove the residual solvents. Four solvents including dichloromethane (DCM), tetrahydrofuran (THF), toluene, and *o*-DCB were utilized for the vapor annealing; for *o*-DCB it was heated to 50 °C in order to generate enough vapors because of its low vapor pressure at room temperature. Figure 2 shows the respective transfer and output characteristics of OFETs with thin films of **P1**, **P2**, and **P3** after exposure to vapors of different solvents. As listed in Table S2, hole mobilities of thin films of **P1** increased albeit slightly, compared to those of as-prepared thin-film and that after thermal annealing at 80 °C, after vapor-annealing with four solvents. Interestingly, hole mobilities of thin films of **P2** and **P3** increase to 0.024 and 0.135 $\text{cm}^2 \text{ V}^{-1} \text{ s}^{-1}$, which are about 12 and 45 times those of their respective thin films after thermal annealing, after annealing with vapors of DCM and *o*-DCB, respectively. The threshold voltages and on/off ratios keep almost unaltered after solvent vapor annealing for thin films of **P1** and **P2** (see Table S2). Obvious enhancement in hole mobility was also detected for thin films of **P2** after exposure to vapors of THF, toluene, and *o*-DCB in comparison with thermal annealing. But, hole mobilities of thin films of **P3** after solvent vapor annealing with DCM, THF, and toluene are in the same order with that after thermal annealing (see Table S2). This may be blamed to the extremely poor solubility of **P3** in toluene, THF, and DCM. To conclude, hole mobilities of **P2** and **P3** can be remarkably enhanced after vapor annealing with

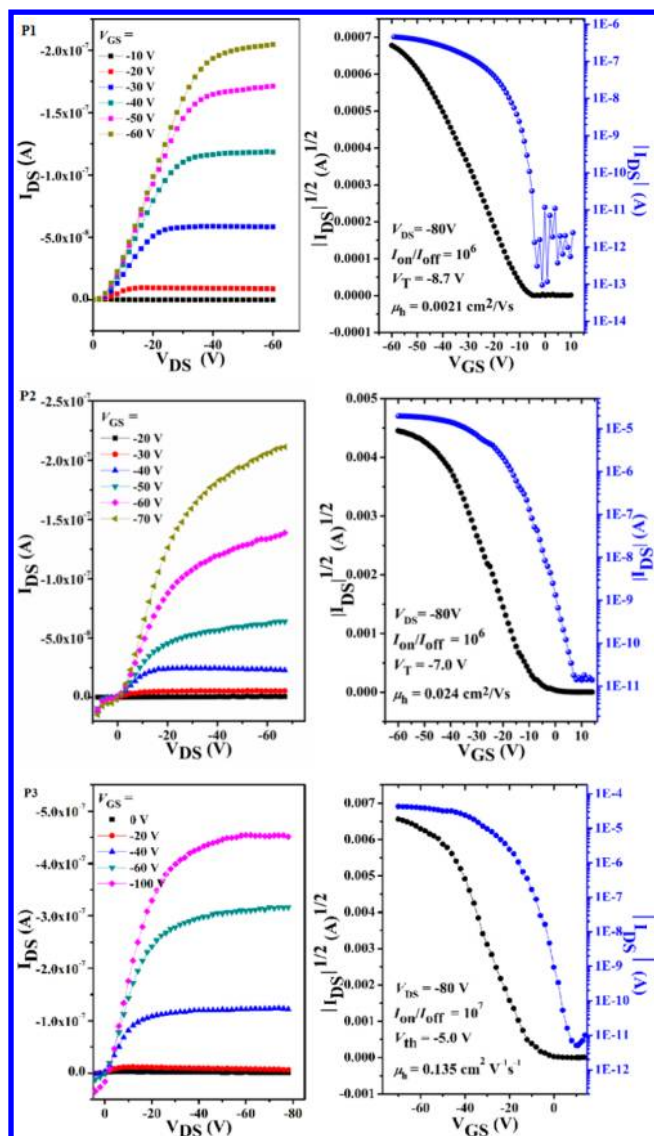


Figure 2. Typical output and transfer characteristics of OTFTs of **P1**, **P2**, and **P3**; OTFTs devices were solvent vapor annealed for 24 h with DCM, DCM, and *o*-DCB, respectively; the channel width (*W*) was 1440 μm for all OFETs, and the length (*L*) was 50, 5, and 10 μm for OTFTs with thin films of **P1**, **P2**, and **P3**, respectively.

appropriate solvents. As to be discussed below, such solvent vapor annealing may induce rearrangements of conjugated polymers within their thin films²¹ and accordingly improve morphologies of their thin films (in particular for **P2** and **P3**) which may be responsible for improving hole transporting according to previous reports.²² The performances of OFETs with thin films of **P1**, **P2**, and **P3** after solvent vapor annealing were measured after being left in air for certain times. For instance, the hole mobility and on/off ratio were just slightly reduced after the OFET with thin film of **P3** was left in air for 8 days (see Figure S5). Similar results were also detected for OFETs with thin films of **P2** and **P3**. Such air stability agrees well with HOMO energies (around -5.40 eV) of **P1**, **P2**, and **P3**.

AFM and XRD Studies. Thin films of **P1**, **P2**, and **P3** were characterized with AFM after thermal and solvent vapor annealing. Figure 3 shows the respective AFM images of thin films of **P1**, **P2**, and **P3** after thermal treatment and exposure to

vapors of appropriate solvents. For thin film of **P1**, the surface morphology was not altered largely after thermal and solvent annealing with DCM; domains of different sizes were formed after thermal annealing, and relatively large domains were also generated after exposure to DCM vapors. But, the morphology of thin-film of **P1** became nonuniform and domains were not well interconnected. These agrees well with the observation that hole mobility of thin film of **P1** is not high and is not obviously affected by thermal and solvent vapor annealing.

The as-prepared thin films of **P2** and **P3** were obviously not uniform and domains were not interconnected as depicted in Figure 3. However, domains within thin films of **P2** and **P3** started to merge to form large domains after the respective thermal annealing. This is consistent with the fact that hole mobilities of thin films of **P2** and **P3** increase slightly after thermal annealing (see Table S2). Even larger and continuous domains were generated after solvent vapor annealing with DCM and *o*-DCB, respectively (see Figure 3). Such thin-film morphological changes are in agreement with the remarkable enhancement of hole mobilities for thin films of **P2** and **P3** after solvent vapor annealing (see Table S2).

XRD analysis was also conducted for as-prepared thin films of **P1**, **P2**, and **P3** and those after thermal and solvent vapor annealing. As depicted in Figure S4, no sharp diffraction peaks were detected for their thin films even after thermal and solvent vapor annealing. These XRD data reveal that conjugated backbones and side chains of **P1**, **P2**, and **P3** are not orderly arranged within their thin films. This agrees well with the fact that hole mobilities of thin films of these polymers are not high. Further investigations to improve order degrees within thin films of these conjugated polymers are under way.

CONCLUSION

Three new alternating conjugated D–A polymers **P1**, **P2**, and **P3** featuring a new electron-accepting framework derived from NDI were successfully prepared and characterized. These conjugated polymers are thermally stable under 325 $^{\circ}\text{C}$. Their HOMO/LUMO energies are -5.39 to -5.43 eV and -3.58 to -3.59 eV, respectively, based on their absorption spectra and redox potentials. OFETs with thin films of **P1**, **P2**, and **P3** were fabricated with conventional techniques. They exhibit p-type semiconducting behavior, and their hole mobilities increase slightly after thermal annealing. Notably, hole mobilities of thin films of **P2** and **P3** are remarkably enhanced after solvent vapor annealing, reaching 0.024 and 0.135 $\text{cm}^2 \text{V}^{-1} \text{s}^{-1}$, respectively. Such mobility enhancement is in agreement with the surface morphological alterations for thin films of **P1**, **P2**, and **P3** based on AFM studies. These studies manifest that the new large conjugated framework (1 in Scheme 2) derived from NDI is promising for constructing conjugated polymers toward optoelectronic materials. Further studies include variation of electron-donating moieties and side chains as well as the linking moieties to construct new alternating D–A conjugated polymers toward new semiconductors and photovoltaic materials.

EXPERIMENTAL SECTION

DBNDI was synthesized according to previous reports.²³ The synthesis of (5-bromothiophen-2-yl)ethynyl)copper was described in the Supporting Information.

Synthesis of Compound 3. DBNDI (492 mg, 0.50 mmol), (5-bromothiophen-2-yl)ethynyl)copper (500 mg, 2.0 mmol), and 20 mL of DMSO were heated at 130 $^{\circ}\text{C}$ under a N_2 atmosphere for 2.0 h.

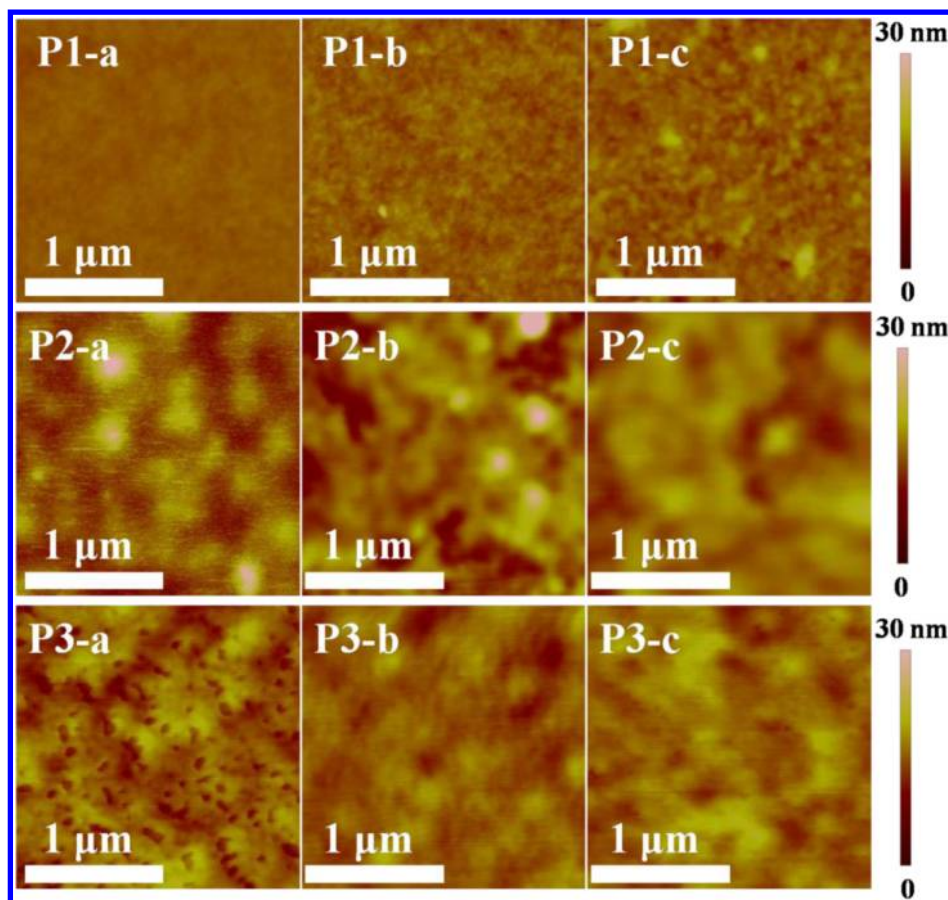


Figure 3. AFM images of thin films of **P1**, **P2**, and **P3**: as-prepared films (**P1-a**, **P2-a**, **P3-a**); after thermal annealing at 80, 100, and 140 °C, respectively (**P1-b**, **P2-b**, **P3-b**); after solvent vapor annealing with DCM, DCM, and *o*-DCB, respectively (**P1-c**, **P2-c**, **P3-c**).

After cooling to room temperature, purple-red solids were separated by filtration and subjected to flash column chromatography with CH_2Cl_2 /petroleum ether (60–90 °C) (v/v, 1/1.5) as eluent to afford **3** as purple-red solids (405 mg) in 68% yield. ^1H NMR (400 MHz, CDCl_3): δ 8.69 (s, 2H), 7.27 (d, J = 3.9 Hz, 2H), 7.06 (d, J = 3.9 Hz, 2H), 4.12 (d, J = 7.2 Hz, 4H), 1.99 (s, 2H), 1.42 – 1.22 (m, 64H), 0.87 – 0.83 (q, J = 6.7 Hz, 12H). ^{13}C NMR (100 MHz, CDCl_3): 162.27, 161.67, 136.58, 135.17, 130.89, 126.52, 126.35, 125.16, 124.89, 124.41, 117.13, 95.30, 95.14, 45.01, 32.07, 30.21, 29.85, 29.84, 29.81, 29.51, 22.83, 14.27. MS (MALDI-TOF): m/z 1197.5 ($M + 1$)⁺. Anal. Calcd for $\text{C}_{66}\text{H}_{88}\text{Br}_2\text{N}_2\text{O}_4\text{S}_2$: C, 66.20; H, 7.41; N, 2.34; S, 5.36. Found: C, 66.38; H, 7.40; N, 2.37; S, 5.56.

Synthesis of Compound 1. Compound **3** (360 mg, 0.30 mmol) was dissolved in 20 mL of dry CH_2Cl_2 , then TFSIH (bis-(trifluoromethane) sulfonamide) (340 mg, 0.12 mmol) was added, and the solution was stirred at room temperature under a N_2 atmosphere for 4.0 h. Then, after removal of solvents compound **2** was obtained as blue solids which were used for the next step without further purification. To a dry CH_3OH solution (25 mL) of compound **2** $\text{NH}_3\cdot\text{H}_2\text{O}$ (1.25 mL, 14.7 mmol) was added. The color immediately changed from blue to red, and the solution was refluxed for 1.0 h. Then, the mixture was diluted with water (30 mL) and extracted with CH_2Cl_2 (3 \times 20 mL). The organic layer was dried with MgSO_4 and concentrated by rotary evaporation. The crude was purified by silica gel column chromatograph with CH_2Cl_2 /petroleum ether (60–90 °C) (v/v, 1/1.5) as eluent to give **1** as red solids (185.5 mg) in 52% yield. ^1H NMR (400 MHz, CDCl_3): δ 8.71 (s, 2H), 7.70 (s, 2H), 7.41 (d, J = 3.9 Hz, 2H), 7.09 (d, J = 3.9 Hz, 2H), 4.40 (d, J = 7.2 Hz, 4H), 2.08 (s, 2H), 1.24 – 1.17 (m, 64H), 0.85 – 0.78 (m, 12H). ^{13}C NMR (100 MHz, CDCl_3): 161.70, 149.00, 146.99, 146.16, 134.80, 131.40, 128.07, 125.42, 125.01, 121.27, 116.33, 109.05, 109.00, 46.15, 32.06, 32.03, 29.86, 29.78, 29.49, 22.82, 22.79, 14.25. MS (MALDI-TOF): m/z

1195.5 ($M + 1$)⁺. Anal. Calcd for $\text{C}_{66}\text{H}_{90}\text{Br}_2\text{N}_4\text{O}_2\text{S}_2$: C, 66.31; H, 7.59; N, 4.69; S, 5.36. Found: C, 66.48; H, 7.54; N, 4.66; S, 5.48.

General Synthetic Procedures of P1, P2, and P3. Compound **1** (1.0 equiv), the corresponding bis-trimethylstannane compound (1.0 equiv), and $\text{P}(o\text{-tolyl})_3$ (0.08 equiv) were dissolved in toluene (for **P1** and **P2**) or chlorobenzene (for **P3**) (15 mL). The solution was purged with N_2 for 30 min, and then $\text{Pd}_2(\text{dba})_3$ (0.04 equiv) was added. The reaction was stirred at 110 °C for 2 days. Then, a toluene or chlorobenzene solution of tributyl(phenyl)stannane was added, and the mixture was stirred for an additional 2.0 h, followed by the addition of a few drops of bromobenzene and further stirring for 2.0 h. The resulting mixture was poured into methanol and stirred for 3.0 h. The dark precipitates were filtered off and subjected to Soxhlet extraction for 2 days successively with methanol, hexane, and acetone for the removal of remaining monomers, oligomers, and catalytic impurities. For **P1** and **P2**, the remaining polymers were redissolved in chloroform and precipitated again after addition of methanol; the precipitates were filtered, washed with methanol, and dried under vacuum at 50 °C. For **P3**, the remaining polymer was suspended in 50 mL of *o*-dichlorobenzene and heated at 100 °C for 12 h. Then, the hot solution was filtered, and the solution of **P3** was collected; precipitates were filtered after addition of methanol, washed with methanol, and dried under vacuum at 50 °C.

For the Synthesis of P1. Compound **1** (183 mg, 0.15 mmol), the corresponding bis-tin compound (169 mg, 0.15 mmol), $\text{P}(o\text{-tolyl})_3$ (3.7 mg, 0.012 mmol), and $\text{Pd}_2(\text{dba})_3$ (5.5 mg, 0.006 mmol) were used. **P1** was obtained as red solids (205 mg) in 74% yield. ^1H NMR (400 MHz, CDCl_3): δ 9.00 (br), 7.61–7.41 (br), 7.05–6.84 (br), 4.75 (br), 4.09–3.93 (br), 2.54–2.11 (br), 1.15–1.12 (br), 0.76 (m). ^{13}C NMR (100 MHz, solid state): δ 161.83, 149.95, 147.15, 144.43, 143.72, 138.29, 135.88, 132.07, 128.05, 127.06, 116.25, 113.39, 110.83, 109.58, 32.51–30.56, 23.49, 14.71. M_w/M_n (GPC) = 82 500/28 600.

Anal. Calcd for $C_{114}H_{170}N_4O_4S_4$: C, 76.54; H, 9.58; N, 3.13; S, 7.17. Found: C, 75.73; H, 9.53; N, 2.95; S, 6.92.

For the Synthesis of P2. Compound **1** (143 mg, 0.12 mmol), the corresponding bis-tin compound (102 mg, 0.12 mmol), $P(o\text{-tolyl})_3$ (3.0 mg, 0.009 mmol), and $Pd_2(dba)_3$ (4.4 mg, 0.0048 mmol) were used. **P2** was obtained as red solids (170 mg) in 93% yield. 1H NMR (400 MHz, $CDCl_3$): δ 9.07 (br), 7.52 (br), 7.18–7.00 (br), 5.13–4.88 (br), 2.68–0.85 (br). ^{13}C NMR (100 MHz, Solid state): δ 162.51, 150.03, 148.53, 146.94, 145.86, 144.12, 140.24, 136.61, 127.25, 117.15, 109.43, 45.40, 30.68, 23.58, 14.82. M_w/M_n (GPC) = 94 200/28 600. Anal. Calcd for $C_{100}H_{142}N_4O_2S_4$: C, 76.97; H, 9.17; N, 3.59; S, 8.22. Found: C, 76.35; H, 9.07; N, 3.48; S, 8.03.

For the Synthesis of P3. Compound **1** (130 mg, 0.11 mmol), the corresponding bis-tin compound (45 mg, 0.11 mmol), $P(o\text{-tolyl})_3$ (2.8 mg, 0.0088 mmol), and $Pd_2(dba)_3$ (4.1 mg, 0.0044 mmol) were used. **P3** was obtained as red solids (72 mg) in 60% yield. 1H NMR (300 MHz, *o*-dichlorobenzene, 100 °C): δ 9.49 (br), 8.15 (br), 7.33 (br), 5.46 (br), 2.87–0.68 (br). ^{13}C NMR (100 MHz, solid state): δ 161.82, 156.59, 147.36–143.05, 137.31, 135.16, 126.90–122.17, 109.49, 104.67, 46.77, 30.62, 23.59, 14.97. M_w/M_n (GPC) = 56 600/29 200. Anal. Calcd for $C_{70}H_{92}N_4O_2S_3$: C, 75.22; H, 8.30; N, 5.01; S, 8.61. Found: C, 74.75; H, 8.20; N, 4.74; S, 8.33.

■ ASSOCIATED CONTENT

■ Supporting Information

General information, TGA and DSC analysis, calculated molecular orbitals, XRD patterns, details of the OTFTs fabrication and performance data, 1H NMR and ^{13}C NMR spectra. This material is available free of charge via the Internet at <http://pubs.acs.org>.

■ AUTHOR INFORMATION

Corresponding Author

*E-mail: gxzhang@iccas.ac.cn (G.Z.), dqzhang@iccas.ac.cn (D.Z.).

Notes

The authors declare no competing financial interest.

■ ACKNOWLEDGMENTS

The present research was financially supported by NSFC, the State Basic Program and Chinese Academy of Sciences.

■ REFERENCES

- (1) (a) Wang, C.; Dong, H.; Hu, W.; Liu, Y.; Zhu, D. *Chem. Rev.* **2012**, *112*, 2208. (b) Shiota, Y.; Kageyama, H. *Chem. Rev.* **2007**, *107*, 953. (c) Cheng, Y.; Yang, S.; Hsu, C. *Chem. Rev.* **2009**, *109*, 5868. (d) Bernius, M. T.; Inbasekaran, M.; O'Brien, J.; Wu, W. *Adv. Mater.* **2000**, *12*, 1737. (e) Mei, J.; Kim, D. H.; Ayzner, A. L.; Toney, M. F.; Bao, Z. *J. Am. Chem. Soc.* **2011**, *133*, 20130. (f) Henson, Z. B.; Müllen, K.; Bazan, G. C. *Nat. Chem.* **2012**, *4*, 699. (g) Xu, Y.; Chueh, C.; Yip, H.; Ding, F.; Li, Y.; Li, C.; Li, X.; Chen, W.; Jen, A. K. Y. *Adv. Mater.* **2012**, *24*, 6356. (h) Durban, M. M.; Kazarinoff, P. D.; Segawa, Y.; Luscombe, C. K. *Macromolecules* **2011**, *44*, 4721. (i) Li, H.; Mei, J.; Ayzner, A.; Toney, M.; Tok, J.; Bao, Z. *Org. Electron.* **2012**, *13*, 2450. (j) Schubert, M.; Dolfen, D.; Frisch, Roland, S.; Steyrlleuthner, R.; Stillner, B.; Chen, Z.; Scherf, U.; Koch, N.; Facchetti, A.; Neher, D. *Adv. Energy Mater.* **2012**, *2*, 369.
- (2) (a) Grimsdale, A. C.; Chan, K. L.; Martin, R. E.; Jokisz, P. G.; Holmes, A. B. *Chem. Rev.* **2009**, *109*, 897. (b) Kamtekar, K. T.; Monkman, A. P.; Bryce, M. R. *Adv. Mater.* **2010**, *22*, 572.
- (3) (a) Li, Y. *Acc. Chem. Res.* **2012**, *45*, 723. (b) Arias, A. C.; MacKenzie, J. D.; McCulloch, I.; Rivnay, J.; Salleo, A. *Chem. Rev.* **2010**, *110*, 3. (c) Ning, Z.; Fu, Y.; Tian, H. *Energy Environ. Sci.* **2010**, *3*, 1170. (d) Chen, J.; Cao, Y. *Acc. Chem. Res.* **2009**, *42*, 1709. (e) Huang, F.; Chen, K.; Yip, H.; Hau, S.; Acton, O.; Zhang, Y.; Luo, J.; Jen, A. K. Y. *J. Am. Chem. Soc.* **2009**, *131*, 13886. (f) Guo, X.; Zhou, N.; Lou, S.; Hennek, J.; Ortiz, R.; Butler, M.; Boudreault, P.; Strzalka, J.; Morin, P.; Leclerc, M.; Navarrete, T.; Ratner, M.; Chen, L.; Chang, R.; Facchetti, A.; Marks, T. J. *J. Am. Chem. Soc.* **2012**, *134*, 18427. (g) Huang, Y.; Guo, X.; Liu, F.; Huo, L.; Chen, Y.; Russell, T.; Han, C.; Li, Y.; Hou, J. *Adv. Mater.* **2012**, *24*, 3383. (h) Yang, T.; Wang, M.; Duan, C.; Hu, X.; Huang, L.; Peng, J.; Huang, F.; Gong, X. *Energy Environ. Sci.* **2012**, *5*, 8208. (i) Son, H.; Carsten, B.; Jung, I.; Yu, L. *Energy Environ. Sci.* **2012**, *5*, 8158. (j) Würthner, F.; Meerholz, K. *Chem.—Eur. J.* **2010**, *16*, 9366.
- (4) (a) Beaujuge, P. M.; Fréchet, J. M. J. *J. Am. Chem. Soc.* **2011**, *133*, 20009. (b) Takimiya, K.; Shinamura, S.; Osaka, I.; Miyazaki, E. *Adv. Mater.* **2011**, *23*, 4347. (c) Ajayaghosh, A.; George, S. J. *J. Am. Chem. Soc.* **2001**, *123*, 514. (d) Chen, L.; Hernandez, Y.; Feng, X.; Müllen, K. *Angew. Chem., Int. Ed.* **2012**, *51*, 7640. (e) Osaka, I.; Shinamura, S.; Abea, T.; Takimiya, K. *J. Mater. Chem. C* **2013**, *1*, 1297. (f) Andreasen, J.; Pisula, W.; Müllen, K.; Cornil, J.; Beljonne, D. *Adv. Mater.* **2013**, *25*, 1939. (g) Niedzialek, D.; Lemaire, V.; Dudenko, D.; Shu, J.; Hansen, M.; Beaujuge, P. M.; Tsao, H.; Hansen, M.; Amb, C.; Risko, C.; Subbiah, J.; Choudhury, K.; Mavrinskiy, A.; Pisula, W.; Bredas, J.; So, F.; Müllen, K.; Reynolds, J. *J. Am. Chem. Soc.* **2012**, *134*, 8944. (h) Zhou, W.; Wen, Y.; Ma, L.; Liu, Y.; Zhan, X. *Macromolecules* **2012**, *45*, 4115. (i) Liu, S.; Li, H.; Shi, M.; Jiang, H.; Hu, X.; Li, W.; Fu, Lei; Chen, H. *Macromolecules* **2012**, *45*, 9004.
- (5) (a) Li, Y.; Sonar, P.; Singh, S. P.; Zeng, W.; Soh, M. S. *J. Mater. Chem.* **2011**, *21*, 10829. (b) Li, Y.; Sonar, P.; Singh, S. P.; Soh, M. S.; van, M. M.; Tan, J. *J. Am. Chem. Soc.* **2011**, *133*, 2198. (c) Li, Y.; Singh, S. P.; Sonar, P. *Adv. Mater.* **2010**, *22*, 4862. (d) Gao, X.; Di, C.; Hu, Y.; Yang, X.; Fan, H.; Zhang, F.; Liu, Y.; Li, H.; Zhu, D. *J. Am. Chem. Soc.* **2010**, *132*, 3697. (e) Zhao, Y.; Di, C.; Gao, X.; Hu, Y.; Zhang, L.; Liu, Y.; Wang, J.; Hu, W.; Zhu, D. *Adv. Mater.* **2011**, *23*, 2448. (f) Deng, Y.; Chen, Y.; Zhang, X.; Tian, H.; Bao, C.; Yan, D.; Geng, Y.; Wang, F. *Macromolecules* **2012**, *45*, 8621.
- (6) (a) Ha, J. S.; Kim, K. H.; Choi, D. H. *J. Am. Chem. Soc.* **2011**, *133*, 10364. (b) Lee, J. S.; Son, S. K.; Song, S.; Kim, H.; Lee, D. R.; Kim, K.; Ko, M. J.; Choi, D. H.; Kim, B.; Cho, J. H. *Chem. Mater.* **2012**, *24*, 1216. (c) Subramanian, S.; Kim, F.; Ren, G.; Li, H.; Jenekhe, S. A. *Macromolecules* **2012**, *45*, 9029. (d) Lei, T.; Dou, J.; Pei, J. *Adv. Mater.* **2012**, *24*, 6457.
- (7) (a) Chen, H. Y.; Hou, J.; Zhang, S.; Liang, Y.; Yang, G.; Yang, Y.; Yu, L.; Wu, Y.; Li, G. *Nat. Photonics* **2009**, *3*, 649. (b) Zhou, H.; Yang, L.; Stuart, A. C.; Price, S. C.; Liu, S.; You, W. *Angew. Chem., Int. Ed.* **2011**, *50*, 2995.
- (8) (a) Szarko, J. M.; Guo, J.; Liang, Y.; Lee, B.; Rolczynski, B. S.; Strzalka, J.; Xu, T.; Loser, S.; Marks, T. J.; Yu, L.; Chen, L. X. *Adv. Mater.* **2010**, *22*, 5468. (b) Dou, L.; You, J.; Yang, J.; Chen, C. C.; He, Y.; Murase, S.; Moriarty, T.; Emery, K.; Li, G.; Yang, Y. *Nat. Photonics* **2012**, *6*, 180.
- (9) (a) Zhan, X. W.; Tan, Z. A.; Domercq, B.; An, Z. S.; Zhang, X.; Barlow, S.; Li, Y. F.; Zhu, D. B.; Kippelen, B.; Marder, S. R. *J. Am. Chem. Soc.* **2007**, *129*, 7246. (b) Tan, Z. A.; Zhou, E. J.; Zhan, X. W.; Wang, X.; Li, Y. F.; Barlow, S.; Marder, S. R. *Appl. Phys. Lett.* **2008**, *93*, 073309. (c) Popere, B. C.; Della Pelle, A. M.; Thayumanavan, S. *Macromolecules* **2011**, *44*, 4767. (d) Wang, J.; Chen, X.; Cai, Z.; Luo, H.; Li, Y.; Liu, Z.; Zhang, G.; Zhang, D. *Polym. Chem.* **2013**, DOI: 10.1039/c3py00129f. (e) Cai, Z.; Guo, Y.; Yang, S.; Peng, Q.; Luo, H.; Liu, Z.; Zhang, G.; Liu, Y.; Zhang, D. *Chem. Mater.* **2013**, *25*, 471.
- (10) (a) Zhou, E.; Cong, J.; Wei, Q.; Tajima, K.; Yang, C. H.; Hashimoto, K. *Angew. Chem., Int. Ed.* **2011**, *50*, 2799. (b) Chen, Z.; Lee, M. J.; Ashraf, R. S.; Gu, Y.; Albert-Seifried, S.; Meedom Nielsen, M.; Schroeder, B. T.; Anthopoulos, D.; Heeney, M.; McCulloch, I.; Sirringhaus, H. *Adv. Mater.* **2012**, *24*, 647. (c) Kronemeijer, A. J.; Gili, E.; Shahid, M.; Rivnay, J.; Salleo, A.; Heeney, M.; Sirringhaus, H. *Adv. Mater.* **2012**, *24*, 1558. (d) Beaujuge, P. M.; Ellinger, S.; Reynolds, J. R. *Nat. Mater.* **2008**, *7*, 795.
- (11) (a) Liu, W. J.; Zhou, Y.; Ma, Y. G.; Cao, Y.; Wang, J.; Pei, J. *Org. Lett.* **2007**, *9*, 4187. (b) Lei, T.; Cao, Y.; Fan, Y.; Liu, C.-J.; Yuan, S.-C.; Pei, J. *J. Am. Chem. Soc.* **2011**, *133*, 6099. (c) Guo, X.; Zhang, M.; Huo, L.; Cui, C.; Wu, Y.; Hou, J.; Li, Y. *Macromolecules* **2012**, *45*, 6930. (d) Zhang, Y.; Zou, J.; Cheuh, C.; Yip, H.; Jen, A. K.-Y. *Macromolecules* **2012**, *45*, 5427. (e) Lei, T.; Dou, J.; Ma, Z.; Yao, C.; Liu, C.; Wang, J.

Pei, J. *J. Am. Chem. Soc.* **2012**, *134*, 20025. (f) Lei, T.; Cao, Y.; Zhou, X.; Peng, Y.; Bian, J.; Pei, J. *Chem. Mater.* **2012**, *24*, 1762.

(12) (a) Kim, F. S.; Guo, X.; Watson, M. D.; Jenekhe, S. A. *Adv. Mater.* **2010**, *22*, 478. (b) Yang, D.; Kim, K.; Cho, M.; Jin, J.; Choi, D. *Polym. Sci.* **2013**, *51*, 1457.

(13) (a) Yuen, J. D.; Kumar, R.; Zakhidov, D.; Seifter, J.; Lim, B.; Heeger, A. J.; Wudl, F. *Adv. Mater.* **2011**, *23*, 3780. (b) Steckler, T. T.; Zhang, X.; Hwang, J.; Honeyager, R.; Ohira, S.; Zhang, X.-H.; Grant, A.; Ellinger, S.; Odom, S. A.; Sweat, D.; Tanner, D. B.; Rinzler, A. G.; Barlow, S.; Bredas, J.-L.; Kippelen, B.; Marder, S. R.; Reynolds, J. R. *J. Am. Chem. Soc.* **2009**, *131*, 2824.

(14) (a) Chen, Z.; Zheng, Y.; Yan, H.; Facchetti, A. *J. Am. Chem. Soc.* **2009**, *131*, 8. (b) Yan, H.; Chen, Z.; Zheng, Y.; Newman, C.; Quinn, J. R.; Dötz, F.; Kastler, M.; Facchetti, A. *Nature* **2009**, *457*, 679. (c) Baeg, K.; Khim, D.; Jung, S.; Kang, M.; You, I.; Kim, D.; Facchetti, A.; Noh, Y. *Adv. Mater.* **2012**, *24*, 5433.

(15) (a) Guo, X.; Watson, M. D. *Org. Lett.* **2008**, *10*, 5333. (b) Guo, X.; Kim, F. S.; Seger, M. J.; Jenekhe, S. A.; Watson, M. D. *Chem. Mater.* **2012**, *24*, 1434.

(16) Babel, A.; Jenekhe, S. A. *J. Am. Chem. Soc.* **2003**, *125*, 13656.

(17) Li, Y.; Zhang, G.; Yang, G.; Guo, Y.; Di, C.; Chen, X.; Liu, Z.; Liu, H.; Xu, Z.; Xu, W.; Fu, H.; Zhang, D. *J. Org. Chem.* **2013**, *78*, 2926.

(18) Ryu, D.; Corey, E. J. *J. Am. Chem. Soc.* **2003**, *125*, 6388.

(19) (a) Kondo, M.; Uchikawa, M.; Namiki, K.; Zhang, W.; Kume, S.; Nishibori, E.; Suwa, H.; Aoyagi, S.; Sakata, M.; Murata, M.; Kobayashi, Y.; Nishihara, H. *J. Am. Chem. Soc.* **2009**, *131*, 12112. (b) Kondo, M.; Uchikawa, M.; Kume, S.; Nishihara, H. *Chem. Commun.* **2009**, 45, 1993. (c) Rao, K.; Kusamoto, T.; Toshimitsu, F.; Inayoshi, K.; Kume, S.; Sakamoto, R.; Nishihara, H. *J. Am. Chem. Soc.* **2010**, *132*, 12472. (d) Kondo, M.; Uchikawa, M.; Zhang, W.; Namiki, K.; Kume, S.; Murata, M.; Kobayashi, Y.; Nishihara, H. *Angew. Chem., Int. Ed.* **2007**, *46*, 6271.

(20) The regions between 0.50 and 0.75 V in the CV curves of **P1**, **P2**, and **P3** are rather slightly higher than the respective baselines. This may be blamed to the trace amounts of impurities from either solvents or electrode surfaces.

(21) Solvent vapor annealing was utilized to enhance the performances of OTFTs, which was ascribed to improve the film morphologies yielding larger grains with perhaps better crystallinity: (a) Dickey, K. C.; Anthony, J. E.; Loo, Y.-L. *Adv. Mater.* **2006**, *18*, 1721. (b) Lee, W. H.; Kim, D. H.; Cho, J. H.; Jang, Y.; Lim, J. A.; Kwak, D.; Cho, K. *Appl. Phys. Lett.* **2007**, *91*, 092105.

(22) (a) Meng, H.; Bao, Z.; Lovinger, A. J.; Wang, B. C.; Mujsce, A. M. *J. Am. Chem. Soc.* **2001**, *123*, 9214. (b) Wu, Y.; Li, Y.; Gardner, S.; Ong, B. S. *J. Am. Chem. Soc.* **2005**, *127*, 614.

(23) Chaignon, F.; Falkenström, M.; Karlsson, S.; Blart, E.; Odobel, F.; Hammarström, L. *Chem. Commun.* **2007**, 43, 64.